Check for updates

AGU100 ADVANCING EARTH AND SPACE SCIENCE

Geophysical Research Letters

RESEARCH LETTER
10.1029/2018GL081473

Conditions for the Long-Term Preservation of a Deep Brine Reservoir in Ceres

Julie C. Castillo-Rogez[1], M. A. Hesse[2], M. Formisano[3], H. Sizemore[4], M. Bland[5], A. I. Ermakov[1], and R. R. Fu[6]

[1]Jet Propulsion Laboratory, California Institute of Technology, Pasadena, CA, USA, [2]Department of Geological Sciences, The University of Texas at Austin, Austin, TX, USA, [3]INAF-IAPS, Istituto di Astrofisica e Planetologia Spaziali di Roma, Italy, [4]Planetary Science Institute, Tucson, AZ, USA, [5]United States Geological Survey, Flagstaff, AZ, USA, [6]Department of Earth and Planetary Sciences, Harvard University, Cambridge, MA, USA

Key Points:
- Brines can be preserved in Ceres if the crust is enriched in clathrate hydrates
- Lateral variations in clathrate content can drive variations in surface heat flux and topography response

Supporting Information:
- Supporting Information S1

Correspondence to:
J. C. Castillo-Rogez,
julie.c.castillo@jpl.nasa.gov

Citation:
Castillo-Rogez, J. C., Hesse, M. A., Formisano, M., Sizemore, H., Bland, M., Ermakov, A. I., & Fu, R. R. (2019). Conditions for the long-term preservation of a deep brine reservoir in Ceres. *Geophysical Research Letters*, *46*, 1963–1972. https://doi.org/10.1029/2018GL081473

Received 29 NOV 2018
Accepted 1 FEB 2019
Accepted article online 5 FEB 2019
Published online 19 FEB 2019

Abstract We propose a new internal evolution model for the dwarf planet Ceres matching the constraints on Ceres' present internal state from the Dawn mission observations. We assume an interior differentiated into a volatile-dominated crust and rocky mantle, and with remnant brines in the mantle, all consistent with inferences from the Dawn geophysical observations. Simulations indicate Ceres should preserve a warm crust until present if the crust is rich in clathrate hydrates. The temperature computed at the base of the crust exceeds 220 K for a broad range of conditions, allowing for the preservation of a small amount of brines at the base of the crust. However, a temperature ≥250 K, for which at least 1 wt.% sodium carbonate gets in solution requires a crustal abundance of clathrate hydrates greater than 55 vol.%, a situation possible for a narrow set of evolutionary scenarios.

Plain Language Summary We search internal evolution models of dwarf planet Ceres that match the observations returned by the Dawn mission. A key feature to be reproduced is the long-term persistence of liquid below the crust, at about 40 km depth, as suggested by the observed topography. The possibility for the occurrence of liquid in Ceres at present depends on the presence of insulating material in the crust, for example, in the form of gas hydrates. The latter are also suggested from geophysical and geological observations and geochemical modeling. Our modeling shows in these conditions that liquid can be preserved for a wide range of evolutionary scenarios.

1. Introduction

Per its combination of chemical, physical, and geological observations on global, regional, and local scales, the Dawn mission has provided the most extensive data set for a water-rich body (Russell et al., 2016). Ceres is 940-km large with a mean density of 2,162 kg/m^3 (Park et al., 2016). This corresponds to a water to rock ratio of 47:53 in volume or 25:75 in mass, simply assuming all the water is in the form of ice and rock is anhydrous. Hence, Ceres' evolution is driven by the interplay of radiogenic heating with the thermodynamic and mechanical properties of water ice and hydrated minerals. Observational constraints returned by the Dawn mission are summarized in recent studies (e.g., McCord & Castillo-Rogez, 2018). The geophysical properties this study aims to match are summarized in section 2. They include constraints on the properties of the upper 100 km, in particular composition and viscosity profile. An important feature derived from Dawn's observations is a rapid decrease in viscosity within the uppermost 40 km and persistent low viscosities at about 10^{21} Pa s below and at least down to 100 km depth. This has been interpreted by the presence of a few vol.% pore fluid (Fu et al., 2017). Our objective is to determine what set of starting conditions and assumptions on the properties of the crust and potassium distribution enable the preservation of fluids at about 40 km depth until present. Methods are presented in section 3 and results in section 4. These results provide thermal context for various processes whose occurrence has been suggested for Ceres, in particular the prospect for cryovolcanism and the development of cryomagma reservoirs upon impact heating in the crust (Hesse & Castillo-Rogez, 2019, hereafter referred to as HC19; section 5). In turn, this study brings new insights into the internal evolution of a body, which, from a geophysical standpoint, is relevant to other midsized dwarf planets and icy moons.

©2019. American Geophysical Union. All Rights Reserved.

2. Constraints on Ceres' Interior From Dawn

In the course of 3 years of orbital mapping, the Dawn mission returned images, near-infrared spectra, elemental abundances, and gravity measurements of Ceres on a global scale. Gravity data yielded a normalized mean moment of inertia of about 0.37 pointing to partial differentiation (Park et al., 2016). Admittance analysis provided additional constraints on crustal properties, which is 40 km thick on average with a density of 1,200 to 1,400 kg/m^3 (assuming a two layer model, Ermakov et al., 2017). The crust overlays a mantle with a density of ~2,400 kg/m^3 and a viscosity lower than 10^{21} Pa s, which Fu et al. (2017) interpreted as evidence for a small amount of pore fluid. The nature of the fluid is not constrained but it could realistically be sodium and potassium chloride brines as suggested by geochemical modeling (Castillo-Rogez et al., 2018; Neveu & Desch, 2015). The brines likely correspond to residual liquid from the freezing of a global ocean suggested in Ceres early on (Ammannito et al., 2016; Castillo-Rogez & McCord, 2010). The eutectic temperature of that brine could be as low as about 220 K (Castillo-Rogez et al., 2018). Ammonia could also be present and decrease the eutectic further. However, the widespread occurrence of ammonium both in the form of clays and salts on Ceres' surface indicates these formed in an environment where ammonia was a minor component. Following Le Chatelier's Principle, most of the ammonia should be turned into ammonium since the latter was removed from the medium, either by exchange with cations in clays or by salt precipitation.

Extensive evidence for the occurrence of salt compounds in Ceres' crust is expressed in the form of many sites enriched in carbonates and ammonium chlorides (De Sanctis et al., 2018). These species are likely associated with other chlorides, like hydrohalite (Castillo-Rogez et al., 2018) that cannot be detected by Dawn's instruments. Brines are believed to play a role in the emplacement of two outstanding geological landmarks: Ahuna Mons (Ruesch et al., 2016) and the bright material (faculae) in Occator crater (De Sanctis et al., 2016; Quick et al., 2019). Both constructs display sodium carbonate (De Sanctis et al., 2016, for the Occator faculae and Zambon et al., 2017, for Ahuna Mons). The deep brine layer identified by Fu et al. (2017) has been suggested as a reservoir for the Occator faculae (Quick et al., 2019).

Additional constraints on Ceres' crustal composition come from its mechanical strength, which Bland et al. (2016) found to be at least three orders of magnitude greater than water ice for Ceres' temperatures. It suggests no more than 40 vol.% of a weak phase, which Bland et al. (2016) interpreted as an upper bound on the water ice fraction. That fraction could be less if the crust also contains void porosity. The extent of porosity is not constrained though and might show lateral variations, as indicated by the distribution of surface fractures (Scully et al., 2017). Strong phases are required to reproduce the strength of the crust, which Fu et al. (2017) inferred to be a mixture of phyllosilicates, salt hydrates, and gas hydrates (i.e., clathrate hydrates). The latter are likely to be mixed methane and carbon dioxide hydrates (Castillo-Rogez et al., 2018) with a density of about 1,000 kg/m^3 (Waite et al., 2007). Geochemical modeling suggests there should be no more than 20 vol.% salts in the crust and the averaged density of these salts, composed of carbonates and chlorides, is about 2,200 kg/m^3 (Castillo-Rogez et al., 2018). In this framework, phyllosilicates are a mixture of magnesium serpentine and clays, consistent with surface composition (De Sanctis et al., 2018). A mixture of 10 vol.% silicates, 20 vol.% hydrated salts, and 30 vol.% ice and 40 vol.% clathrates matches the average crustal density derived by Ermakov et al. (2017) and is consistent with the strength estimates from Bland et al. (2016) and Fu et al. (2017). Recent experimental work (Qi et al., 2018) suggests that the fraction of strong phases in Ceres' crust might not need to be more than ~6 vol.%, if it is in the form of fine particles forming bands between ice grains. Hence, an endmember composition may not include any clathrate. However, contrarily to the inference by Qi et al. (2018) that Ceres' crust may contain up to 90 vol.% ice, the density constraint still requires up to 30 vol.% of a dense phase such as silicates and salts.

Ceres' crust relaxes on scales greater than ~250 km, which Fu et al. (2017) interpreted with a crustal viscosity profile decreasing by one order of magnitude every 10 km. Formisano et al. (2018) used a 2-D finite element numerical code to solve the thermal convection equations in the Boussinesq approximation and explored the onset of subsolidus thermal convection in Ceres' crust. They found that no thermal convection is possible, assuming less than 40 vol.% of weak material. Convection may be possible if the ice content is slightly greater than 40% and the temperature at the base of the crust ranges from 250 to 300 K. Strong thermal convection is possible if 50 vol.% of ice is assumed, leading to a Rayleigh number greater than 10^8. However, as shown below, the modeled temperatures at the base of the crust are expected to be colder than required for convection to be initiated throughout Ceres' history. Hence we assume heat is transferred by conduction in Ceres' crust.

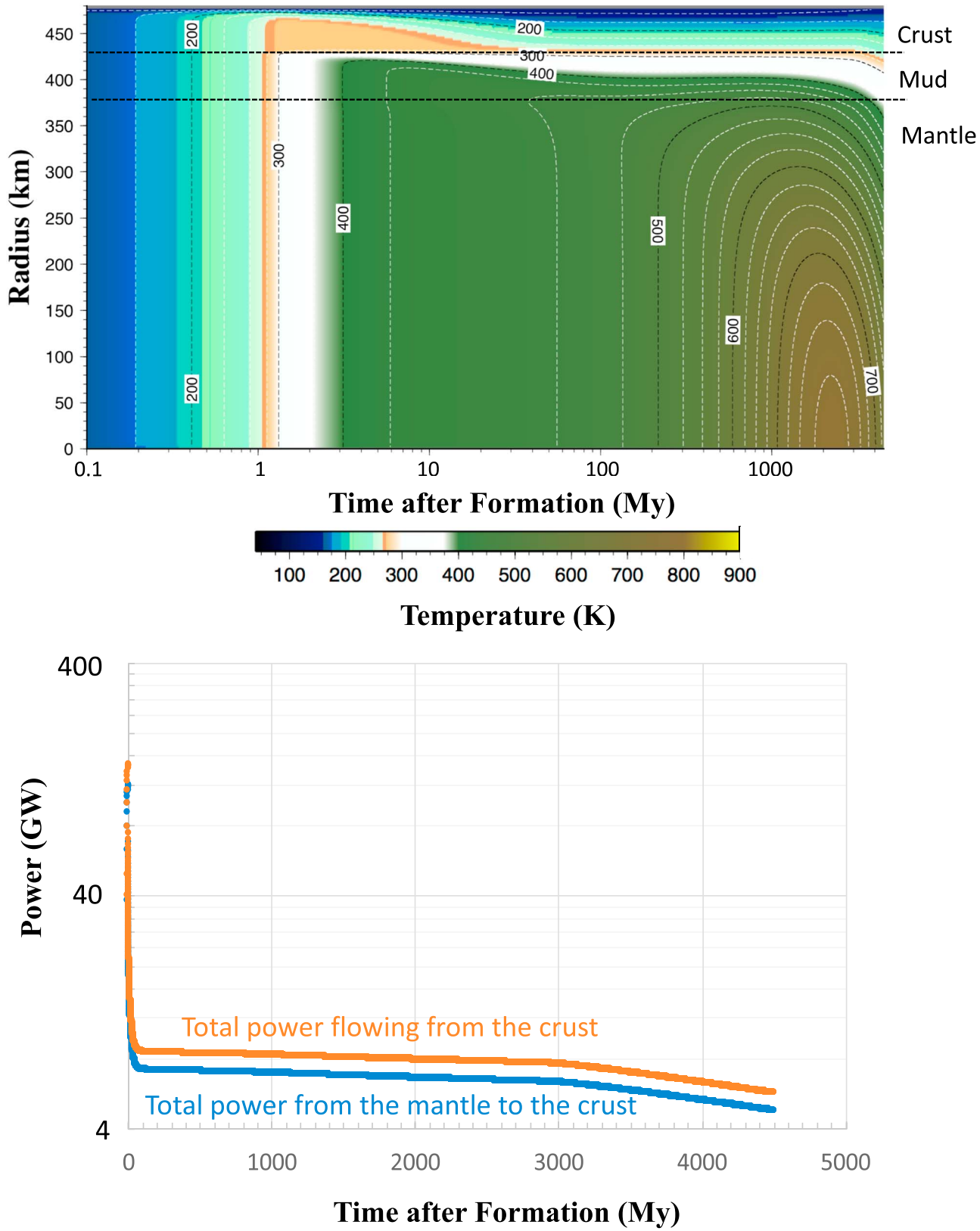

Figure 1. (a) Representative modeling of Ceres' thermal evolution for a time of formation of 3.5 Ma after the production of Ca-Al inclusions, a clathrate abundance in the crust of 50 vol%, a mantle thermal conductivity of 1.5 W/m/K, and loss of 50% of ^{40} from the rock. Contour labels are temperatures in Kelvin. The figures display isotherms every 25 K. (b) Corresponding heat flow evolution integrated over the rocky mantle surface at 430 km radius and Ceres' surface for a mean radius of 470 km.

3. Modeling Approach

This paper follows the one-dimensional thermal modeling approach by Castillo-Rogez and Lunine (2010). We account for the redistribution of potassium following leaching from the silicates upon aqueous alteration. This process is promoted in presence of ammonium whose exchange with potassium and sodium is enhanced at temperature below 50 °C (Neveu et al., 2017). In Castillo-Rogez et al. (2018), potassium accumulates with chlorine and sodium in the residual liquid layer at the base of the crust. The distribution of this brine may encompass a few tens of kilometers in the upper part of the mantle or a larger area depending on porosity. We vary the fraction of potassium leached from the rock from 10% to 90% and redistribute it in the brine layer in the upper part of the mantle, down to the 100-km depth (i.e., the upper 60 km of the mantle) that could be probed by the Fu et al. (2017) modeling.

Ceres is assumed to form about 3.5 Ma after the condensation of calcium and aluminum rich inclusions, which define the starting concentrations of ^{26}Al in Ceres. The exact time of formation is not important for this study as long as there is enough ^{26}Al to drive global melting and differentiation following formation. For times of formation later than 5 Ma after calcium and aluminum rich inclusions, Castillo-Rogez and McCord (2010) found that Ceres could preserve a thick (>150 km) crust of its original composition, presumably of dry rock. This situation is not consistent with the Dawn observations, both in terms of surface composition, crustal density, and moment of inertia and we do not cover it in the present study. For the initial concentration in long-lived radioisotopes, we chose a mean carbonaceous chondrite composition characterized by an average potassium content of ~500–550 μg/g (Lodders, 2003).

Freezing occurs top down and results in the development of a crust that is ice rich. Modeling of the freezing of the ocean with FREZCHEM (Marion et al., 2010) yields salts and clathrates (Castillo-Rogez et al., 2018). Clathrates may represent the dominant form of water at pressures of a few MPa. Hence, the crustal composition may range from the minimal 30 vol.% clathrates required by the observations (on top of silicates and hydrated salts) up to 70 vol.%. The averaged thermal conductivity of the mixture, K_{crst} ranges from about 0.7 W/m/K for 0 vol.% ice (i.e., 70 vol.% clathrates) to 2.4 W/m/K for 0 vol.% clathrates. Silicates are a minor component of the mixture, and thus their impact on the thermal conductivity is small; see the supporting information, for example, Dai et al. (2015), Durham et al. (2010), Grimm and Mcween Jr (1989), Grindrod et al. (2008), Muraoka et al. (2014), Opeil et al. (2010), Schofield et al. (2014), Waite et al. (2007) for the material properties used in the modeling and the methodology for computing thermal conductivity (De Vries, 1952; Fricke, 1924; Hamilton & Crosser, 1962).

Settling of phyllosilicates upon melting of the ice is assumed to proceed to near completion except for a 60 km layer at the interface between the crust and solid mantle that is enriched in briny fluid. That is, we do not model a mudball interior, in which silicate grains remain in suspension with a fluid phase throughout much of the early mantle (Travis et al., 2018). The rationale for this choice is that assumption on the fraction of rocky particles that can remain in suspension in the ocean widely vary. For example, ionic charging, a common phenomenon observed in marine clays (e.g., Sutherland et al., 2015) and experimental work specific to Ceres (Cannon & Britt, 2019) could play a major role in driving particle settling, or flocculation, as the ocean freezes and thus salinity increases. Furthermore, muddy sediment is difficult to erode and resuspend (Hjulstrom, 1935). The mudball model predicts the long-term preservation of hundreds of kilometers of liquid inside Ceres at present and, presumably, could match the mechanical constraints derived by Fu et al. (2017). Our admittedly simpler model yields higher heat flow and thus provides a bound on the maximum temperatures that can be reached in Ceres at present. So, the two approaches may be viewed as two endmember evolutionary pathways for Ceres.

Lastly, the concentration of metal-rich, that is, dense, particles toward the center cannot be ruled out (King et al., 2018). However, the extent of that process is unconstrained, so this study assumes a simple three-layer structure (crust, brine-rich rocky layer, and solid mantle) for Ceres' interior. This modeling does not account for organics, which might be abundant in the crust (Marchi et al., 2018). Organics are diverse and their densities cover a broad range, but their abundance in Ceres' crust is not constrained.

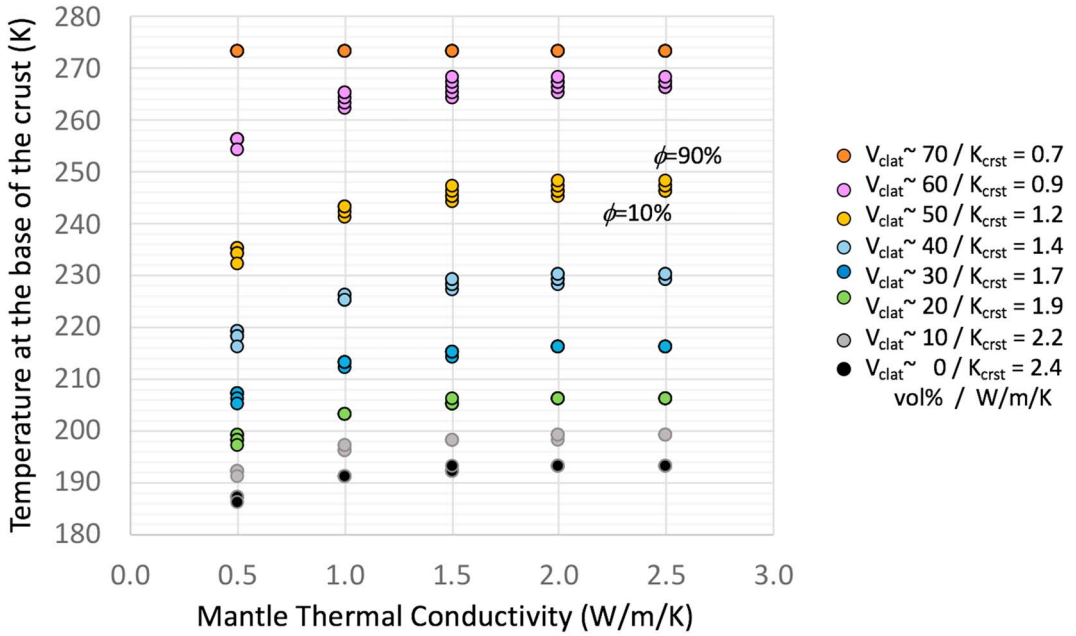

Figure 2. Temperature at the base of the crust as a function of the thermal conductivity of the mantle (assumed constant) and of the averaged temperature in the crust, which is a function of the volume fraction of clathrate hydrates, assuming a mixture of 20 vol.% hydrated salts, 10 vol.% phyllosilicates, the rest being ice and clathrates. Point spreads for each model represents the impact of potassium removal from the rock and its concentration in a 60-km thick brine layer below the crust, assuming ϕ = 10% to 90% transfer of potassium from the rock to the brine.

4. Representative Interior Evolution Models Consistent With Dawn's Observations

The model presented in Figure 1a is characterized by a mantle thermal conductivity of 1.5 W/m/K, an averaged crust thermal conductivity of 1.2 W/m/K (corresponding to 50 vol.% clathrates), and assumes 50% of the potassium has been leached from the silicates and is stored in remaining liquid at the top (60 km) of the mantle. In these conditions, the mantle remains cool and never reaches the dehydration temperature of serpentine and clays, around 800 K. This is consistent with the inference of a low density mantle by Ermakov et al. (2017), as, once initiated, dehydration generally encompasses a large fraction of the mantle (Castillo-Rogez & McCord, 2010).

Figure 1b shows the total heat power flowing out of the core crust as a function of time for that model. Due to the low conductivity of the core and the insulating effect of the crust, heat leaks out slowly with only ~16 vol.% more loss at the surface than supply from the core.

Trends in parametric dependence (Figure 2) show that the key parameter determining the temperature at the base of the crust is, as expected, the crustal thermal conductivity. The mantle thermal conductivity, which determines the heat flowing from the mantle to the crust, further contributes to warming the base, although its impact is at most 16 K over a factor five increase. Hence, efficient heat transfer from the mantle combined with an insulating effect of the crust results in trapping heat at the base of the crust and yields temperatures above 220 K (i.e., the eutectic of the chloride brine mixture) for a large set of conditions, specifically if $K_{crst} \leq$ ~1.4 W/m/K (i.e., ≥40 vol.% clathrates). The crust-mantle interface temperature reaches the water eutectic for $K_{crst} \leq$0.8 W/m/K (i.e., ≥65 vol.% clathrates), whereas an ice-dominated crust with an average thermal conductivity ≥1.6 W/m/K (i.e., ≥35 vol.% clathrates) prevents temperatures warm enough for brines to persist until present.

The contribution of the displacement of ^{40}K from the rock to a brine layer at the top of the mantle results in increasing the temperature at the interface with the crust by only a few degrees.

A low value of K_{crst} can be explained if the crust is enriched in hydrates, such as clathrate hydrates. An averaged conductivity of 1.4 W/m/K corresponds to about 40 vol.%, which, combined with 20 vol.% salts and 10 vol.% silicates (to meet the observed crustal density), is consistent with the crustal strength derived by

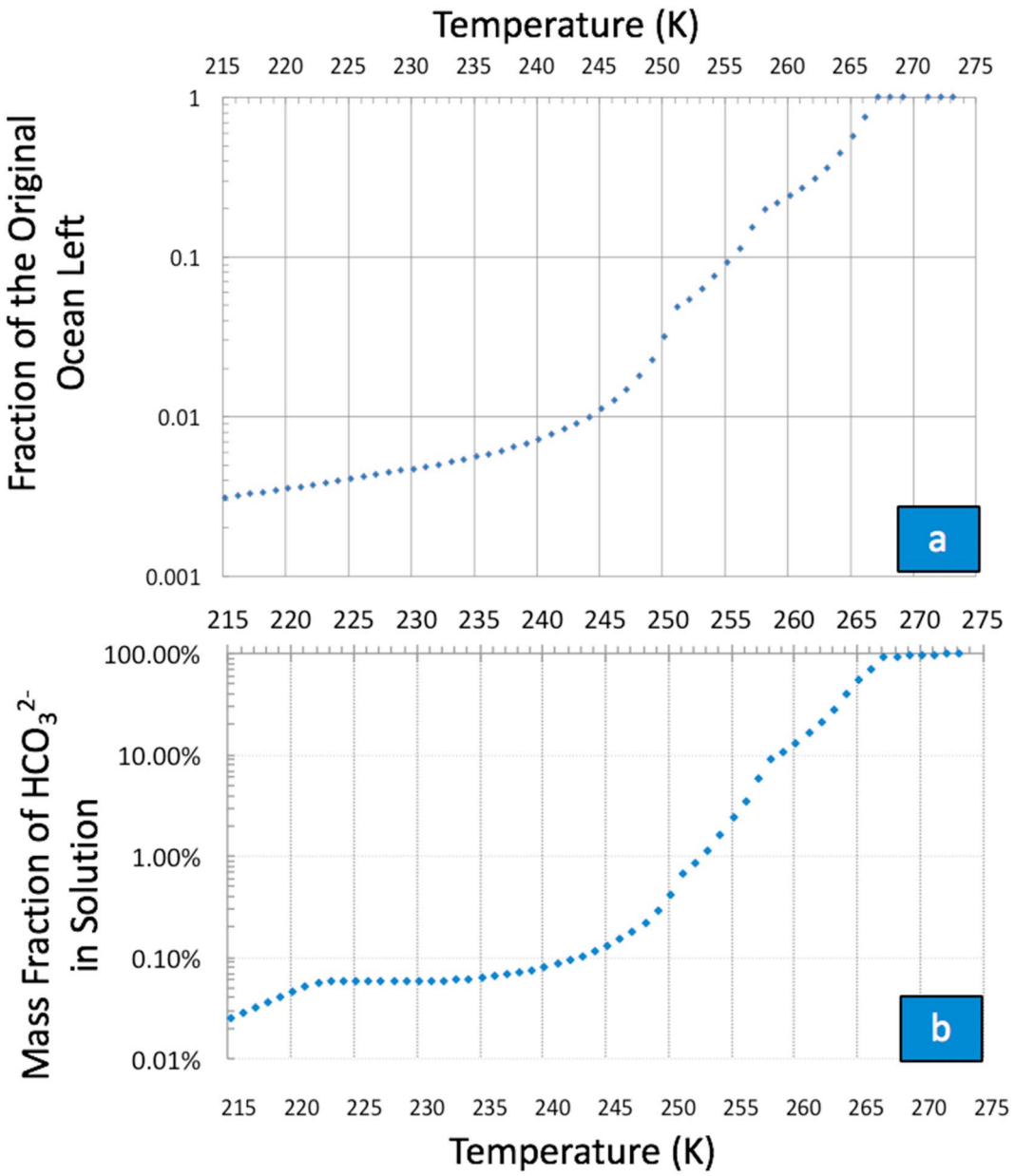

Figure 3. (a) Fraction of liquid left assuming the original ocean was 60 km thick (following settling of the hydrated rock mantle), as a function of the temperature at the base of the crust, taking as a reference the ocean composition evolution model from Castillo-Rogez et al. (2018). (b) Fraction of bicarbonate ion in solution as a function of temperature taking as a reference the ocean evolution model from Castillo-Rogez et al. (2018).

Bland et al. (2016). An average value of 0.8 W/m/K requires ~65 vol.% clathrate hydrates, which is theoretically possible from the standpoint of the Fu et al. (2017) and Bland et al. (2016) geological constraints but implies that clathrate hydrates formed during the freezing of the ocean avoided destabilization produced by impacts. This scenario is hard to reconcile with Ceres' impacting history and with regional evidence for increased ice content in the crust (Sizemore et al., 2019). On the other hand, $K_{crst} \geq 1.6$ W/m/K, the condition for Ceres to be entirely frozen at present, implies scarce clathrates, ≤35 vol.%, which is also a plausible scenario. Increased abundance of silicates with respect to hydrated salts, two high strength materials of similar densities but contrasting thermal conductivities, can further act in increasing thermal conductivity.

Temperatures in the modeled mantle exceed the dehydration temperature of hydrated silicates when the average thermal conductivity of the mantle $K_{mtl} \leq 1.2$ W/m/K. Dehydration then encompasses a large

volume of the mantle (>300 km, see also Castillo-Rogez & McCord, 2010) and thus is not consistent with the average mantle density of ~2,400 kg/m^3 inferred by Ermakov et al. (2017).

The amount of remaining liquid versus temperature for the mix of salts predicted by Castillo-Rogez et al. (2018) is presented in Figure 3a. The remaining liquid fraction represents ≤2% of the original ocean for temperatures below ~248 K and ≤1% below ~244 K. At 220 K, only 0.4% of the original ocean remains. Assuming that all of Ceres' volatile content melted as a consequence of short-lived radioisotope decay (Castillo-Rogez & McCord, 2010), these fractions correspond to a global layer between 200 and 1,000 m thick. However, below the crust, this liquid is likely distributed in a matrix of silicates and other solid materials in the form of pore (interstitial) fluid down to at least 100 km depth. Further modeling is required to determine the distribution of the liquid based on the expected matrix properties (e.g., porosity and permeability).

5. Implications and Discussion

Our modeling shows that it is realistic from a thermal standpoint to expect at least a few vol.% of brines to be preserved in Ceres' mantle until present, provided that the crust is enriched in insulating material such as clathrates. Clathrates are expected from geochemical modeling (Castillo-Rogez et al., 2018) and may also be responsible for the inferred low density and high mechanical strength of the crust (Bland et al., 2016; Fu et al., 2017). However, unless the crust is dominated by clathrates, Ceres is on the edge of being completely frozen, which is also consistent with Neveu and Desch (2015). On the other hand, our modeling approach potentially yields a conservative case in comparison to the mudball model (Travis et al., 2018). The bottom line is that the preservation of liquid inside Ceres until present is expected for a wide range of thermal evolution scenarios.

Lateral Variations in Crustal Properties: Sizemore et al. (2019) inferred lateral variations in ice content across Ceres. In particular, the Hanami Planum region displays Ceres' most ancient terrains and mildly relaxed geological features in comparison to the surrounding planitiae. Most of the craters with central pits are concentrated in this region. Hanami Planum is also characterized by a thicker crust than average (~50 km, Ermakov et al., 2017). A possible interpretation is that this old region has preserved a substantial fraction of clathrates with respect to the planitiae that might represent basins created by large impacts (Marchi et al., 2016). Variable clathrate abundance could locally shift the average crustal thermal conductivity from <1 to > 2 W/m/K, with potential signatures in the geology that remain to be explored. Combining a thicker crust with a low thermal conductivity could then lead to locally warmer temperatures and thus increase abundance in liquid at the base of the crust. Preliminary estimates suggest the base of Hanami Planum could be ~5–10 K warmer than the average basal temperature over scales that cannot be resolved by the Fu et al. (2017) topography relaxation study. However, two- or three-dimensional thermal modeling is required for a more accurate estimate.

Prospect for Cryovolcanism: Ahuna Mons, a ~4-km high by 17-km wide construct, sits on a ~40-km thick crust, similar to our modeling assumption, that is, temperatures colder than 245 K are expected at the base of the crust in that region. Even in the most optimistic case, the current basal heat flow is lower than 3 mW/m^2, insufficient to drive convective upwelling (Formisano et al., 2018). The lack of flexural deformation associated with the mons also indicates a low heat flow. Instead, Neveu and Desch (2015) suggested that expressions of volcanism on Ceres' surface could result from passive upwelling of mantle material due to volume changes in a freezing interior. A model that reconciles both mineralogy and geophysics remains to be pursued. Other cryovolcanic constructs (Sori et al., 2018) could have been produced by differential loading following impacts in a heterogeneous crust (Bland et al., 2018).

The occurrence of sodium carbonate at both the Occator faculae and Ahuna Mons implies the sources of these constructs to be warm enough for that compound to be in solution. The fluid does not require a large concentration of sodium carbonate though, since the bulk of the Occator dome and of Ahuna Mons could be built from a different material, for example, ice shielded from sublimation by a thin crust of carbonate and chlorides. For our average model, the fraction of $NaHCO_3$ in solution is only 0.1 wt.% at 245 K (Figure 3b). Temperatures in excess of 250 K are required for several percent of that compound to be in solution. Such warm temperatures could be met below Hanami Planum, as noted in the previous subsection. Sodium carbonate is a minor component of the salt inventory modeled for Ceres (e.g., in comparison to the chlorides) and is predicted to be among the first salts incorporated in the crust (Castillo-Rogez et al., 2018). Thus, the extent to which the deep brine layer could represent a major reservoir of sodium carbonate for the Occator faculae is uncertain. An alternative, and potentially complementary scenario is that geological activity

associated with Occator and other large craters (in the past) was in part driven by the heat produced upon impacting, which represents an additional way to inject heat into the crust and put in solution sodium carbonates already present in the crust (HC19). A hybrid model combining both impact-generated melt and a deeper source is another possibility (see next subsection).

Thermal Context for Impact Melt Production: Our modeling can be used to compute the amount and depth of melt produced by impacts throughout Ceres' history. In the case of the Occator faculae, a cryomagma reservoir produced by impact heat (Bowling et al., 2019; HC19) can reach the required temperature for a significant fraction of crustal sodium carbonate to get in solution and contribute to the bulk of the facula carbonates as the solution is brought to the surface from freezing stresses (following a similar process as described in Quick et al., 2019). The thermal gradient inferred from our modeling is at least four times steeper than the thermal gradient assumed by Bowling et al. (2019). The thermal background determines the size of the original melt chamber (i.e., the warmer the chamber, the larger the reservoir) and can have a significant effect over the lifetime of that melt (HC19). For example, increasing the clathrate content from 30 to 65 vol.% increases the lifetime of a given chamber size by about a factor two (Figure 3c in HC19), that is, the chamber could survive beyond 10 Ma and potentially still be a source for the recent exposure of brines (Nathues et al., 2017), depending on its original size.

6. Summary

The preservation of a relict ocean in Ceres until present is possible if the crust contains more than 40 vol.% insulating materials, such as hydrated salts and clathrates. This is consistent with geochemical predictions and geophysical observations. A moderate rocky mantle thermal conductivity (~1–2 W/m/K) further contributes to the preservation of a warm brine layer at the base of the crust. On the other hand, the displacement of ^{40}K from the rock to the salts has a relatively minor impact on Ceres' crustal temperature. The water ice melting point is reached if the crust is dominated by clathrate hydrates in excess of 65 vol.%, which might be occurring locally. On the other hand, the prospect of shallow liquid at present, as depicted in Nathues et al. (2017) and Stein et al. (2017), is unlikely based on our geophysical modeling. This implies that the exposure of salts from a brine reservoir might be limited to impacts large enough to connect with the >40-km deep brine layer (e.g., via the introduction of fractures) and/or to create a local melt chamber (Bowling et al., 2019; HC19). Conversely, the warm thermal background resulting from a large abundance of hydrates in the crust implies that brine-driven activity following large impacts must have been common in Ceres' history, as illustrated by the many occurrences of salt deposits associated with fracture in large craters (e.g., Buczkowski et al., 2018; Stephan et al., 2018, see also Stein et al., 2017). Clathrates may further contribute to that process by supplying gas upon destabilization and increasing melt buoyancy (e.g., Quick et al., 2019).

One cannot exclude that warmer basal temperatures could be reached locally, for example, below Hanami Planum's thick crust. Conversely, conversion of clathrates into ice by large impacts could increase the average crust thermal conductivity, with possible expressions in the surface morphology. Two- or three-dimensional thermal modeling is required to explore the evolution of Ceres' complex crust for comparison against surface features.

Acknowledgments
Part of this work has been conducted at the Jet Propulsion Laboratory, California Institute of Technology, under a contract with NASA. Government sponsorship acknowledged. The authors are grateful to the two anonymous reviewers for their thorough feedback and fast turnaround. This manuscript relies entirely on theoretical modeling and the input parameters are listed in the paper and supplementary data.

References

Ammannito, E., De Sanctis, M. C., Ciarniello, M., Frigeri, A., Carrozzo, F. G., Combe, J.-Ph., et al. (2016). Distribution of ammoniated magnesium phyllosilicates on Ceres. *Science*, *353*, aaf4279.

Bland, M. T., Raymond, C. A., Fu, R. R., Schenk, P., Kneissl, T., Pasckert, J. H., et al. (2016). Composition and structure of the shallow subsurface of Ceres revealed by crater morphology. *Nature Geoscience*, *9*, 538–542.

Bland, M. T., Sizemore, H. G., Buczkowski, D. L., Sori, M. M., Raymond, C. A., King, S. D., & Russell, C. T. (2018). Why is Ceres lumpy? Surface deformation induced by solid-state subsurface flow. In *49th Lunar and Planetary Science Conference 19-23 March, 2018*, The Woodlands. Texas LPI Contribution No. 2083 id.1627.

Bowling, T. J., Ciesla, F. J., Davison, T. M., Scully, J. E. C., Castillo-Rogez, J. C., & Marchi, S. (2019). Post-impact thermal structure and cooling timescales of Occator crater on asteroid 1 Ceres. *Icarus*. https://doi.org/10.1016/j.icarus.2018.08.028

Buczkowski, D. L., Sizemore, H. G., Bland, M. T., Scully, J. E. C., Quick, L. C., Hughson, K. H. G., et al. (2018). Floor-fractured craters on Ceres and implications for interior processes. *Journal of Geophysical Research: Planets*, *123*, 3188–3204. https://doi.org/10.1029/2018JE005632

Cannon, K. M., & Britt, D. T. (2019). Into the mire: The behavior of fines in a mud ocean on Ceres and other carbonaceous bodies. In *Lunar and Planetary Science Conference*. LPI Contrib. No. 2132, 2038.

Castillo-Rogez, J. C., & Lunine, J. I. (2010). Evolution of Titan's rocky core constrained by Cassini observations. *Geophysical Research Letters*, *37*, L20205. https://doi.org/10.1029/2010GL044398

Castillo-Rogez, J. C., & McCord, T. B. (2010). Ceres' evolution and present state constrained by shape data. *Icarus*, *205*, 443–459. https://doi.org/10.1016/j.icarus.2009.04.008

Castillo-Rogez, J. C., Neveu, M., McSween, H. Y., Fu, R. R., Toplis, M., & Prettyman, T. H. (2018). Insights into Ceres' evolution from surface composition. *Meteoritics and Planetary Science*, *53*, 1820–1843.

Dai, S., Cha, J.-H., Rosenbaum, E. J., Zhang, W., & Seol, Y. (2015). Thermal conductivity measurements in unsaturated hydrate-bearing sediments. *Geophysical Research Letters*, *42*, 6295–6305. https://doi.org/10.1002/2015GL064492

De Sanctis, M. C., Ammannito, E., Carrozzo, F. G., Ciarniello, M., Giardino, M., Frigeri, A., et al. (2018). Ceres's global and localized mineralogical composition determined by Dawn's Visible and Infrared Spectrometer (VIR). *Meteoritics and Planetary Science*, *53*, 1–22.

De Sanctis, M. C., Raponi, A., Ammannito, E., Ciarniello, M., Toplis, M. J., McSween, H. Y., et al. (2016). Bright carbonate deposits as evidence of aqueous alteration on (1) Ceres. *Nature*, *536*, 54–57.12.

De Vries, D. A. (1952). *The thermal conductivity of granular materials*. Boulevard Malesherbes, Paris, France: Institut International du Froid 177.

Durham, W. B., Prieto-Ballesteros, O., Goldsby, D., & Kargel, J. S. (2010). Rheological and thermal properties of icy materials. *Space Science Reviews*, *153*, 273–298.

Ermakov, A. I., Fu, R. R., Castillo-Rogez, J. C., Raymond, C. A., Park, R. S., Preusker, F., et al. (2017). Constraints on Ceres' internal structure and evolution from its shape and gravity measured by the Dawn spacecraft. *Journal of Geophysical Research: Planets*, *122*, 2267–2293. https://doi.org/10.1002/2017JE005302

Formisano, M., Costanzo, F., Magni, G., & De Sanctis, M. C. (2018). (1) Ceres: Study of thermal convection in the mantle and its mechanical effects. In *42nd COSPAR Scientific Assembly*, Held 14-22 July 2018, in Pasadena, California, USA. Abstract id. B1.1-20-18.

Fricke, H. (1924). A mathematical treatment of the electric conductivity and capacity of disperse systems I. The electric conductivity of a suspension of homogeneous spheroids. *Physical Review*, *24*, 575–587.

Fu, R. R., Ermakov, A., Marchi, S., Castillo-Rogez, J. C., Raymond, C. A., Hager, B. H., et al. (2017). Interior structure of the dwarf planet Ceres as revealed by surface topography. *Earth and Planetary Science Letters*, *476*, 153–164.

Grimm, R. E., & Mcween Jr, H. Y. (1989). Water and the thermal evolution of carbonaceous chondrite parent bodies. *Icarus*, *82*, 244–280.

Grindrod, P. M., Fortes, A. D., Nimmo, F., Feltham, D. L., Brodholt, J. P., & Vocadlo, L. (2008). The long-term stability of a possible aqueous ammonium sulfate ocean inside Titan. *Icarus*, *197*, 137–151.

Hamilton, R. L., & Crosser, O. K. (1962). Thermal conductivity of heterogeneous two-component systems. *Industrial & Engineering Chemistry Fundamentals*, *1*(3), 187–191. https://doi.org/10.1021/i160003a005

Hesse, M., & Castillo-Rogez, J. C. (2019). Thermal evolution of the impact-induced cryomagma chamber beneath Occator crater on Ceres. *Geophysical Research Letters*, *45*, 1–9. https://doi.org/10.1029/2018GL080327

Hjulstrom, F. (1935). Studies of the morphological activity of rivers as illustrated by the River Fyris. *Bulletin of the Geological Institution of the University of Upsala*, *25*, 221–527.

King, S. D., Castillo-Rogez, J. C., Toplis, M. J., Bland, M. T., Raymond, C. A., & Russell, C. T. (2018). Ceres internal structure from geophysical constraints. *Meteoritics & Planetary Science*. https://doi.org/10.1111/maps.13063

Lodders, K. (2003). Solar system abundances and condensation temperatures of the elements. *The Astrophysical Journal*, *591*, 1220. https://doi.org/10.1086/375492

Marchi, S., Ermakov, A. I., Raymond, C. A., Fu, R. R., O'Brien, D. P., Bland, M. T., et al. (2016). The missing large impact craters on Ceres. *Nature Communications*, *7*, 12257.

Marchi, S., Raponi, A., Prettyman, T., De Sanctis, M. C., Castillo-Rogez, J., Raymond, C., et al. (2018). An aqueously altered carbon-rich Ceres. *Nature Astronomy*, *3*, 140–145. https://doi.org/10.1038/s41550-018-0656-0

Marion, G., Mironenko, M., & Roberts, M. W. (2010). FREZCHEM: A geochemical model for cold aqueous solutions. *Computers and Geosciences*, *36*(1), 10–15.

McCord, T. B., & Castillo-Rogez, J. C. (2018). Ceres's internal evolution: The view after Dawn. *Meteoritics & Planetary Science*, *53*, 1778–1792. https://doi.org/10.1111/maps.13135

Muraoka, M., Ohtake, M., Susuki, N., Yamamoto, Y., Suzuki, K., & Tsuji, T. (2014). Thermal properties of methane hydrate-bearing sediments and surrounding mud recovered from Nankai Trough wells. *Journal of Geophysical Research: Solid Earth*, *119*, 8021–8033. https://doi.org/10.1002/2014JB011324

Nathues, A., Platz, T., Thangjam, G., Hoffmann, M., Mengel, K., Cloutis, E. A., et al. (2017). Evolution of Occator Crater on (1) Ceres. *Journal of Geophysical Research: Planets*, *153*, 112. https://doi.org/10.3847/1538-3881/153/3/112

Neveu, M., & Desch, S. J. (2015). Geochemistry, thermal evolution, and cryovolcanism on Ceres with a muddy mantle. *Geophysical Research Letters*, *42*, 10197–10206. https://doi.org/10.1002/2015GL066375

Neveu, M., Desch, S., & Castillo-Rogez, J. (2017). Core cracking and hydrothermal circulation can profoundly affect Ceres' geophysical evolution. *Journal of Geophysical Research: Planets*, *120*, 123–154. https://doi.org/10.1002/2014JE004714

Opeil, C. P., Consolmagno, C. J., & Britt, D. T. (2010). The thermal conductivity of meteorites: New measurements and analysis. *Icarus*, *208*, 449–454.

Park, R., Konopliv, A. S., Bills, B. G., Rambaux, N., Castillo-Rogez, J. C., Raymond, C. A., et al. (2016). Interior structure of dwarf planet Ceres from measured gravity and shape. *Nature*, *537*, 515–517.

Qi, C., Stern, L. A., Pathare, A., Durham, W. B., & Goldsby, D. L. (2018). Inhibition of grain boundary sliding in fine-grained ice by intergranular particles: Implications for planetary ice masses. *Geophysical Research Letters*, *45*, 12,757–12,765. https://doi.org/10.1029/2018GL080228

Quick, L., Buzckowski, D. L., Ruesch, O., Scully, J. E. C., Castillo-Rogez, J. C., Raymond, C. A., et al. (2019). A possible brine reservoir below Occator Crater: Thermal and compositional evolution and formation of the Cerealia Dome and Vinalia Faculae. *Icarus*, *320*, 119–135. https://doi.org/10.1016/j.icarus.2018.07.016

Ruesch, O., Platz, T., Schenk, P., McFadden, L. A., Castillo-Rogez, J. C., Quick, L. C., et al. (2016). Cryovolcanic activity on Ceres. *Science*, *353*, aaf4286.

Russell, C. T., Raymond, C. A., Ammannito, E., Buczkowski, D. L., De Sanctis, M. C., Hiesinger, H., et al. (2016). Dawn arrives at Ceres: Exploration of a small, volatile-rich world. *Science*, *353*, 1008–1010.

Schofield, N., Alsop, I., Warren, J., Underhill, J. R., Lehn, R., Beer, W., & Lukas, V. (2014). Mobilizing salt: Magma-salt interactions. *Geology*, *42*, 599–602. https://doi.org/10.1130/G35406.1

Scully, J. E. C., Buczkowski, D. L., Schmedemann, N., Raymond, C. A., Castillo-Rogez, J. C., King, S. D., et al. (2017). Evidence for the interior evolution of Ceres from geologic analysis of fractures. *Geophysical Research Letters*, *44*, 9564–9572. https://doi.org/10.1002/2017GL075086

Sizemore, H., Schmidt, B., Chilton, H., Hughson, K., Castillo-Rogez, J. C., Sori, M., et al. (2019). A global inventory of ice-related morphological features on dwarf planet Ceres. https://doi.org/10.1111/maps.13135

Sori, M. M., Sizemore, H. G., Byrne, S., Bramson, A. M., Bland, M. T., Stein, N. T., & Russell, C. T. (2018). Cryovolcanic rates on Ceres revealed by topography. *Nature Astronomy*, *2*(12), 946–950. https://doi.org/10.1038/s41550-018-0574-1

Stein, N. T., Ehlmann, B. L., Palomba, E., De Sanctis, M. C., Nathues, A., Hiesinger, H., et al. (2017). The formation and evolution of bright spots on Ceres. *Icarus*. https://doi.org/10.1016/j.icarus.2017.10.014

Stephan, K., Jaumann, R., Wagner, R., De Sanctis, M. C., Palomba, E., Longobardo, A., et al. (2018). Dantu's mineralogical properties–A view into the composition of Cere's crust. *Meteoritics and Planetary Science*, *53*, 1866–1883.

Sutherland, B. R., Barrett, K. J., & Gingras, M. K. (2015). Clay settling in fresh and salt water. *Environmental Fluid Mechanics*, *15*, 147–160.

Travis, B. J., Bland, P., Feldman, W. C., & Sykes, M. (2018). Hydrothermal dynamics in a CM-based model of Ceres. *Meteoritics & Planetary Science*, *53*, 2008–2032.

Waite, W. F., Stern, L. A., Kirby, S. H., Winters, W. J., & Mason, D. H. (2007). Simultaneous determination of thermal conductivity, thermal diffusivity and specific heat in sI methane hydrate. *Geophysical Journal International*, *169*, 767–774. https://doi.org/10.1111/j.1365-246X.2007.03382.x

Zambon, F., Raponi, A., Tosi, F., De Sanctis, M. C., McFadden, L. A., Carrozzo, F. G., et al. (2017). Spectral analysis of Ahuna Mons from Dawn mission's visible and infrared spectrometer. *Geophysical Research Letters*, *44*, 97–104. https://doi.org/10.1002/2016GL071303